Published in final edited form as:
*Cell Stem Cell*. 2012 October 5; 11(4): 541–553. doi:10.1016/j.stem.2012.05.025.

# Coordination of Satellite Cell Activation and Self-Renewal by Par-Complex-Dependent Asymmetric Activation of p38α/β MAPK

**Andrew Troy**[1], **Adam B. Cadwallader**[1], **Yuri Fedorov**[1], **Kristina Tyner**[1,2], **Kathleen Kelly Tanaka**[1], and **Bradley B. Olwin**[1,*]

[1]Department of Molecular, Cellular, and Developmental Biology, University of Colorado, Boulder, CO 80309, USA

## SUMMARY

In response to muscle injury, satellite cells activate the p38α/β MAPK pathway to exit quiescence, then proliferate, repair skeletal muscle, and self-renew, replenishing the quiescent satellite cell pool. Although satellite cells are capable of asymmetric division, the mechanisms regulating satellite cell self-renewal are not understood. We found that satellite cells, once activated, enter the cell cycle and a subset undergoes asymmetric division, renewing the satellite cell pool. Asymmetric localization of the Par complex activates p38α/β MAPK in only one daughter cell, inducing *MyoD*, which permits cell cycle entry and generates a proliferating myoblast. The absence of p38α/β MAPK signaling in the other daughter cell prevents *MyoD* induction, renewing the quiescent satellite cell. Thus, satellite cells employ a mechanism to generate distinct daughter cells, coupling the Par complex and p38α/β MAPK signaling to link the response to muscle injury with satellite cell self-renewal.

## INTRODUCTION

Self-renewal is required to maintain adult stem cell homeostasis. In addition to generating transient amplifying cells committed to tissue maintenance or repair, a population of stem cells must retain the progenitor characteristics to sustain tissue integrity and function (Giebel and Bruns, 2008; Doe, 2008; Zhang et al., 2009; van der Flier and Clevers, 2009). Some adult stem cells accomplish this by an asymmetric division wherein one daughter cell commits to proliferation and eventual differentiation as a transient amplifying cell while the other daughter cell retains the stem cell characteristics (Lin, 2008). The evolutionarily conserved Par complex, composed of Partitioning Defective 3 (PAR-3), Partitioning Defective 6 (PAR-6), and an atypical Protein Kinase C (PKC), establishes polarity in asymmetrically dividing cells (Knoblich, 2008). The Par complex is inherited by only one daughter cell, generating asymmetry and distinct fates between daughter cells (Suzuki and Ohno, 2006; Doe, 2001).



*Correspondence: bradley.olwin@colorado.edu.
[2]Present address: OPX Biotechnologies, 2425 55th Street, Suite 100, Boulder, CO 80301, USA

SUPPLEMENTAL INFORMATION

Supplemental Information for this article includes six figures, two tables, Supplemental Experimental Procedures, and two movies and can be found with this article online at http://dx.doi.org/10.1016/j.stem.2012.05.025.

Satellite cells are a heterogeneous population of cells that are responsible for muscle regeneration and comprise the adult muscle stem cells (Collins et al., 2005; Kuang et al., 2007; Sacco et al., 2008; Tanaka et al., 2009; Hall et al., 2010). In uninjured muscle, mitotically quiescent satellite cells, marked by syndecan-4 and PAX7 expression, reside between the basal lamina and plasma membrane of the muscle fiber (Seale et al., 2000; Cornelison et al., 2001; Yablonka-Reuveni and Rivera, 1994; Mauro, 1961). In response to muscle injury, satellite cells immediately phosphorylate p38α/β MAPK to induce *MyoD* and then enter the cell cycle as a transit amplifying population, referred to as myoblasts (Jones et al., 2005; Zhang et al., 2010), eventually undergoing terminal differentiation and fusing to repair muscle (Schultz and McCormick, 1994).

Recently, subsets of satellite cells have been identified that function as satellite cell stem cells (Kuang et al., 2007; Sacco et al., 2008; Tanaka et al., 2009; Hall et al., 2010). One report identified a subpopulation of satellite-SP cells that express the stem cell markers Lymphocyte antigen 6 complex, locus A (SCA1) and ATP-binding cassette, subfamily G, member 2 (ABCG2), display long-term BrdU retention, and engraft to the satellite cell position more efficiently than satellite cells when injected concurrently with muscle injury (Tanaka et al., 2009). Another report describes a subpopulation of *Myf5* satellite cells that undergo asymmetric divisions, generating *Myf5*+ and *Myf5*–daughter cells (Kuang et al., 2007). Similar cells have been identified in cultures of primary satellite cells where “reserve cells” are mitotically quiescent, express PAX7, are MYOD–, and resist differentiation (Olguin and Olwin, 2004; Zammit et al., 2004). Little more is known regarding whether there are distinct populations of satellite stem cells and when satellite stem cells self-renew.

Here, we show that satellite cells self-renew after an initial cell division following a muscle injury and that the signaling mechanisms regulating satellite cell activation and self-renewal are linked. We propose a model for satellite cell self-renewal that involves asymmetric activation or sequestration of the p38α/β MAPK pathway leading to asymmetric induction of *MyoD*, promoting cell cycle entry in one daughter cell, while the other daughter cell reacquires a quiescent satellite-SP cell phenotype (Tanaka et al., 2009). Furthermore, we provide evidence that the Par complex, consisting of PAR-3 and PKCl, asymmetrically activates the p38α/β MAPK pathway in a PKCλ-dependent manner, regulating the acquisition of distinct daughter cell fates.

## RESULTS

### A Subset of Satellite Cells Exit the Cell Cycle in Culture

Satellite cells function as adult skeletal muscle stem cells, yet the mechanisms involved in their self-renewal are not understood. The generation of “reserve” cells that express PAX7 and little or no detectable MYOD, both on intact myofibers and in dispersed culture, is thought to represent “self-renewal” of satellite cells (Olguin and Olwin, 2004; Zammit et al., 2004). To identify potential reserve cells and their relationship to the previously described BrdU-retaining cells (Shinin et al., 2006; Conboy et al., 2007; Tanaka et al., 2009), we pulse-labeled explanted satellite cells with BrdU immediately after dissection and explant (Figure S1A available online) and quantified the PAX7+ myoblasts at each day for 6 days (6d) in culture. The number of PAX7+ cells in culture increases until day 4, when it begins

to decline and, by 6d of culture, PAX7+ cells make up only a small percentage of the total cells (Figure 1A). If reserve cells are present at the time of explant and are retained in culture as a separate quiescent subpopulation, they should fail to be labeled with BrdU. Under our culture conditions, all PAX7+ explanted satellite cells initially enter the cell cycle and incorporate BrdU, suggesting that a reserve quiescent population is not immediately present (data not shown) (Tanaka et al., 2009). Labeling with BrdU upon explant prior to the first cell division, followed by a 3d chase, reveals a subpopulation (13%) of PAX7+ myoblasts that retain BrdU (Figure 1B), consistent with previous reports (Shinin et al., 2006; Conboy et al., 2007; Tanaka et al., 2009). While the PAX7+, BrdU-retaining cells do not increase in number, they comprise a greater portion of PAX7+ cells following a 4d chase (37%) as increasing numbers of BrdU cells lose *Pax7* expression, express Myogenin, and commit to terminal differentiation (Figure 1C) (Olguin and Olwin, 2004; Olguin et al., 2007).

Retention of BrdU has been attributed to nonrandom DNA strand segregation (Shinin et al., 2006; Conboy et al., 2007; Rocheteau et al., 2012), and thus we employed an alternative technique to determine whether PAX7+ reserve cells exit the cell cycle. To eliminate cycling cells, satellite cell explants were treated with the mitotoxin 1β-arabinofuranosylcytosine (AraC), which incorporates into DNA and inhibits DNA and RNA polymerases, promoting apoptosis in S-phase cells (Furth and Cohen, 1968; Zdunski and Ilan, 1980). Satellite cell explants were treated with AraC for 1d intervals immediately upon explant or at each day in culture for 4 consecutive days followed each time by a 1d chase in the absence of AraC (Figure S1B). Treatment with AraC for the first 24 hr of culture failed to eliminate all cells, as BrdU staining indicated some cells do not enter S-phase until after the first 24 hr of culture (Figure 1D). However, when explanted cells were AraC treated from 1d to 2d or 2d to 3d in culture, all PAX7+ cells were eliminated (Figures 1D and 1G), demonstrating that all explanted satellite cells enter the cell cycle in culture. In contrast, when cultures were treated with AraC from 3d to 4d or from 4d to 5d of culture, a population of AraC-resistant, PAX7+ cells survived (Figures 1D and 1H). The AraC-resistant population appears to be generated during the first cell division following satellite cell explant into culture since the percentage of AraC-resistant cells was not significantly changed when treated with AraC from 3d to 4d or 4d to 5d of culture (Figure 1D).

To unequivocally demonstrate that the AraC-resistant, PAX7+ cells initially enter the cell cycle and to show that AraC-resistant cells are label-retaining cells, we treated cultures with BrdU for the first 48 hr in culture and followed the BrdU treatment with a 24 hr AraC treatment (Figure S1C). The cells were then cultured for an additional 24 hr and the numbers of PAX7+/BrdU+ cells were quantified, demonstrating that the AraC-resistant, PAX7+ population incorporates and retains BrdU after either 5d (Figures 1I and 1J) or 6d (Figures 1I and 1K) in culture. These data are consistent with the conclusion that the AraC-resistant cells and long-term BrdU-retaining cells comprise a single population. Furthermore, this population appears to cycle once prior to cell cycle withdrawal, suggesting that the reserve PAX7+ cells arise following the first satellite cell division in culture and are not retained as quiescent cells upon explant.

### AraC-Resistant, Myofiber-Associated Cells Behave as Quiescent Satellite Cells

Explanting satellite cells in culture removes the satellite cell from its niche, imposing an artificial environment that may affect cell behavior. Therefore, we asked if satellite cells explanted with their associated myofibers exhibit behavior similar to that of satellite cell explants in mass culture. We performed timed AraC treatments for satellite cells on intact myofibers, similar to those described for mass cultures (Figure S1D) and scored for satellite cells using anti-Syndecan-4 antibodies. Syndecan-4 is expressed in satellite cells until fusion (Cornelison et al., 2001), whereas PAX7 protein levels increase upon satellite cell activation and rapidly decline upon Myogenin induction (Olguin and Olwin, 2004). Syndecan-4+ satellite cells on intact myofibers proliferate with a time course similar to that observed in mass cultures where the first division occurs between 36 and 48 hr following explant (Figures 2A and 2B). Subsequent divisions occur rapidly, with cell cycle times no greater than every 10–12 hr (Figures 2A–2C), producing large clones by 4d in culture (Figures 2A and 2C). A large decline in Syndecan-4+ satellite cells occurs by 5d in culture due to fusion with the myofiber (Figure 2A). In agreement with the mass culture data, all Syndecan-4+ satellite cells enter the cell cycle since AraC treatment for the first 48 hr in culture or from 1d to 3d in culture eliminates all Syndecan-4+ myofiber-associated cells (Figures 2D and 2E). However, if cells are AraC treated after the first cell division, from 2d to 4d of culture, an AraC-resistant, Syndecan-4+/Myogenin– population remains (Figures 2D and 2F). When myo-fiber-associated satellite cells are AraC treated from 3d to 5d of culture, two AraC-resistant populations are observed, a Syndecan-4+/Myogenin– population and a Syndecan-4+/Myogenin+ population (Figure 2D and S2A). The Syndecan-4+/Myogenin– population is likely a reserve cell population, while the Myogenin+ population has committed to terminal differentiation and is thus AraC resistant. There is no significant increase in the number of AraC-resistant Syndecan-4+/Myogenin– cells for either treatment, further supporting the observation that quiescent satellite cells are generated during the initial cell division postexplant (Figure 2D).

AraC is a DNA polymerase inhibitor (Furth and Cohen, 1968) but is reported to indirectly introduce chromosomal aberrations in treated cells (Park et al., 1991; Sekizawa et al., 2007). Thus, AraC treatment could potentially alter our estimation of the reserve cell population. To independently verify that explanted satellite cells exit the cell cycle following the first cell division, we marked cells with a viable dye, carboxyfluorescein diacetate succinimidyl ester (CFDA-SE) (Figure S1E). CFDA-SE is cell per-meant, intracellularly esterified, and irreversibly bound to proteins and membranes once internalized (Lyons, 1999). Following CFDA-SE application, subsequent cell divisions reduce the dye intensity 2-fold for each cell division (Lyons, 1999) (Figure 2G). We observed that a 15 min CFDA-SE incubation of 2d myofiber cultures labeled all PAX7+ cells (Figure S2B). After 1d (Figure 2H) or 2d (Figure 2I) of culture in the absence of CFDA-SE, the dye is continuously diluted by cell division; by 3d, CFDA-SE is undetectable in the majority of satellite cells (Figure 2J). After this time, a small number of PAX7+ cells retain intense green fluorescence, suggesting that no subsequent cell divisions ensued in these cells following the initial 15 min CFDA-SE treatment of 2d cultures (Figures 2H–2J).

The reserve or self-renewing population of myofiber-associated satellite cells is characterized by PAX7 immunoreactivity but no detectable MYOD immunoreactivity (Olguin and Olwin, 2004; Zammit et al., 2004). We observed that MYOD is undetectable in the majority of AraC-resistant cells (Figures 2K and 2M), while the majority satellite cells on intact myofibers after 4d in culture are predominately MYOD+ (Figures 2L and 2M) (Cornelison et al., 2001). If the AraC-resistant population represents a satellite cell that has self-renewed, then the AraC-resistant cells should be capable of regenerating a myoblast population indistinguishable from that observed on untreated myofibers that contains a quiescent PAX7+/MYOD–population (Olguin and Olwin, 2004; Zammit et al., 2004). Following a 3d to 5d AraC treatment, myofiber cultures were washed and placed in growth medium for an additional 3d. We noted a 2-fold increase in PAX7+ cells following the recovery from the AraC treatment (Figure 2N) and a recapitulation of the PAX7+/MYOD–, PAX7+/MYOD+, AND PAX7–/MYOD+ cell populations in ratios similar to those observed on untreated myofibers (Figure 2O) (Olguin and Olwin, 2004). Moreover, a 5 hr BrdU pulse prior to fixation revealed that the newly generated PAX7+/MYOD population was BrdU as expected and that the PAX7+/MYOD+ population was predominately proliferative (Figure 2O). Furthermore, the PAX7–/MYOD+ population was predominately postmitotic, reflecting terminal differentiation, consistent with PAX7–/MYOD+ cells on untreated myofibers (Figure 2O). Thus, the AraC-resistant cell behaves as a satellite cell stem cell, capable of self-renewal and generating proliferating myoblasts that commit to terminal differentiation.

## Asymmetry in Satellite Cell Daughters

Since all myofiber-associated satellite cells initially enter the cell cycle, but do not appear as pairs following AraC treatment (Figure 2F), we postulated that these cells arise via an asymmetric division. To initially examine asymmetry, we queried all myofiber-associated cell pairs for MYOD staining following the initial cell division. Of 51 cell pairs scored, the majority show equivalent MYOD immunoreactivity in each daughter cell (Figures 3A and 3C). However, in 12% of cell pairs, MYOD protein was not detectable in one daughter cell while the MYOD levels in the other daughter cell were average or greater than those typical of satellite cells at 2d in culture (Figures 3B and 3C). Assuming the pairs are generated by cell division, we propose that a subset of satellite cells divide asymmetrically during the initial cell division after explant, yielding one PAX7+/MYOD+ daughter cell and one PAX7+/MYOD– daughter cell (Figures S3A–S3D). Furthermore, we propose that the PAX7+/MYOD– daughter is quiescent, is AraC-resistant, retains BrdU, and retains CFDA-SE, similar to the previously described reserve population of satellite cells (Olguin and Olwin, 2004; Zammit et al., 2004; Shinin et al., 2006).

To identify genes potentially regulating asymmetric division, we queried Affymetrix gene chip arrays from FACS-enriched Syndecan-4+ satellite cells obtained from uninjured TA muscles and muscles at 12 hr, 24 hr, and 48 hr postinjury (Tanaka et al., 2009) for the Gene Ontology (GO) terms cell polarity (Figure 3D) and planar cell polarity (Figure 3E). Notable among the transcripts changing expression between these time points are members of the Par complex involved in cell polarity and asymmetric division (Suzuki and Ohno, 2006) and

members of the noncanonical Wnt pathway involved in planar cell polarity, previously implicated in symmetric division of satellite cells (Le Grand et al., 2009).

The Par complex participates in the asymmetric distribution of intracellular proteins and the positioning of the plane of cell division (Suzuki and Ohno, 2006). Members of the Par complex, including *Pard3*, *Pard6a*, and *Prkci*, but not *Prkcz*, are differentially expressed during the first satellite cell division in vivo (Figure 3D). We confirmed by qPCR that members of the Par complex, including PKCλ, are present in satellite cells (Figure S3E). Since AraC-resistant cells were generated during the first cell division in myofiber-associated cultures, we scored myofiber-associated satellite cells (identified by phosphohistone-3 [pH3] immunoreactivity) during their first mitosis for PKCλ asymmetry (Figures 3F–3I). In 16% of dividing myofiber-associated satellite cells, PKCλ appears asymmetric (Figures 3F, 3H, 3I) while PKCλ is uniformly distributed in the majority (70%) of dividing cells (Figures 3F and 3G).

While the majority of dividing satellite cells (74%) displayed very low or undetectable levels of PAR-3 protein (Figures 3J and 3K), we observed that PAR-3 is asymmetric in 13% (Figures 3J, 3M, and 3N) and symmetric in another 13% (Figures 3J and 3L) of dividing myofiber-associated satellite cells. We noted that Syndecan-4 immunoreactivity, while present in both daughter cells, is consistently more intense in prospective daughter cells that will receive either PKCλ or PAR-3 (Figures 3H, 3I, 3M, and 3N). Colocalization of PAR-3 and PKCλ was problematic, since the antibodies to both proteins were produced in rabbits and we could not generate enough data for scoring. However, we did observe that PKCλ and PAR-3 colocalize in dividing cells (Figure S3F).

### PKCλ Signaling Is Required for MyoD Induction and Commitment to Myogenesis

If the Par complex is involved in the asymmetric distribution of MYOD during cell division, the Par complex may play a functional role in myogenesis. PKCλ-mediated phosphorylation is essential for Par complex function in cell polarity and asymmetric division (Tabuse et al., 1998; Lin et al., 2000). Therefore, we reduced PKCλ in the MM14 satellite cell line, which also expresses PKCλ, but not PKCξ (Figures S4A and SB), by transfecting an anti-sense *Pkc*l construct (Figure 4A). The loss or reduction of PKCλ reduces the activity of a *MyoD* transcriptional reporter by 5-fold in both MM14 cells (Figure 4B) and primary satellite cells (Figure 4C) where the MYOD reporter is normally robustly active (Figures 4B–4D). Thus, it appears that PKCλ is necessary for MYOD-dependent transcription and myogenesis. Indeed, cells transfected with the sense *Pkc*λ plasmid differentiate normally (Figure 4F), while those cotransfected with the antisense *Pkc*λ plasmid fail to differentiate (Figures 4E and 4G) and fail to express skeletal-muscle-specific myosin heavy chain (Figures 4E and 4H).

To further assess a role for PKCλ, we measured the activity of the muscle-specific α-cardiac actin promoter in MM14 cells and explanted satellite cells after the knockdown of PKCλ. We found that reduction or elimination of PKCλ dramatically inhibited muscle-specific reporter activity in MM14 cells (Figure 4I) and explants of primary satellite cells (Figure 4J), indicating that PKCλ plays a positive role in myogenic differentiation. PKCλ kinase activity appears to be required as increasing amounts of a plasmid expressing a kinase-inactive form of PKCλ reduced muscle-specific reporter activity (Figure 4K). Thus, our data

support a role for the Par complex in promoting myogenesis via MYOD-dependent transcription.

### p38α/β MAPK Is Asymmetrically Activated in Dividing Satellite Cells

The capacity of AraC-resistant cells to repopulate the quiescent PAX7+/MYOD– reserve cell pool, coupled with our observation of asymmetric MYOD distribution in satellite cell daughter cell pairs, is consistent with the commitment of one daughter (PAX7+/MYOD+) to a proliferating myoblast phenotype and the other to a quiescent satellite cell phenotype (PAX7+/MYOD–). Since activation of p38α/β MAPK pathway is required for satellite cell activation and *MyoD* induction (Jones et al., 2005), which in turn is required for licensing origins of replication for myoblast S-phase entry (Zhang et al., 2010), we asked if p38α/β MAPK was asymmetrically distributed. An anti-p38 antibody showed a uniform distribution of p38α/β MAPK in dividing myoblasts (Figure 5A). Although the active phosphorylated p38α/β MAPK (pp38α/β MAPK) is uniformly distributed in the majority of dividing myoblasts (Figure 5B), we observed asymmetric pp38α/β MAPK in a subset of myofiber-associated cells during the first cell division following explant (Figures 5B–5G), which localizes with a subset of the pan-p38α/β MAPK (Figure 5D). When asymmetric, pp38α/β MAPK colocalizes with asymmetric PAR-3 (Figures 5E and 5F) and asymmetric PKCλ (Figures 5G and 5H). These examples of colocalized asymmetry suggest that in a subset of dividing cells, the Par complex and pp38α/β MAPK are involved in asymmetric accumulation of MYOD to promote a myogenic fate in one daughter cell.

To provide better support for this hypothesis, we employed a proximity ligation assay (PLA) (Pisconti et al., 2010) to ask if endogenous PAR-3 and p38α/β MAPK are in a complex in dividing satellite cells. In the presence of the anti-pp38α/β MAPK antibody and the anti-PAR-3 antibody, we observed abundant complexes in mitotic satellite cells (Figures 6A and 6B) that were asymmetric and localized to the cell membrane adhering to the culture substratum (Figures 6C–6F and Movie S1 available online). Complexes were not observed if the anti-PAR-3 antibody was omitted (Figures 6A and 6G). These observations support the idea that the Par complex is involved in p38α/β MAPK signaling. To test this, we utilized a CHOP reporter that provides a direct readout of p38α/β MAPK signaling (Aguirre-Ghiso et al., 2003; Jones et al., 2005). In the presence of ectopically expressed antisense *Pkc*l, but not a sense control, CHOP reporter activity was reduced by 3-fold (Figure 6H). Moreover, we show that inhibition of p38α/β MAPK signaling represses MYOD-dependent transcription upon addition of the active analogs SB203580 and SB202190, but not when the inactive SB203474 analog is present (Figure 6I). Thus, these assays establish a functional link between the Par complex and MYOD-dependent transcription.

### Par-3 Knockdown Increases Satellite Stem Cell Progenitors

We propose that the Par complex is involved in asymmetric activation or sequestration of p38α/β MAPK during satellite cell division, producing a transit-amplifying myoblast daughter cell. To understand the role of PAR-3 in the regulation of p38α/β MAPK during division, we tested two previously validated shRNAs and identified one that reduces PAR-3 protein 20-fold when ectopically overexpressed (Figures S5A and S5B). While the majority of myofiber-associated satellite cells symmetrically activate p38α/β MAPK during the first

division, a subset asymmetrically localize/activate pp38α/β MAPK (Figures 6J and 6L). When PAR-3 is reduced by ectopic shRNA expression, the majority of cells exhibit very low or undetectable levels of pp38α/β MAPK (Figures 6K and 6M), indicating similar requirements for PAR-3 and PKCλ. We observed no asymmetric pp38α/β MAPK in satellite cells where *Par-3* is knocked down (Figures 6J and 6K). If loss of PAR-3 and asymmetric pp38α/β MAPK is involved in myoblast expansion by asymmetric division, *Par-3* knockdown is expected to enhance the quiescent stem cell popula tion and reduce the numbers of transit amplifying myoblasts. Indeed, when *Par-3* is knocked down, a 16-fold reduction in cell number and a loss of PAX7 cells (Figure 6O) is accompanied by a 5-fold increase in the AraC-resistant progenitor population (Figure 6P), demonstrating a shift from transit amplifying myoblasts to the AraC-resistant satellite stem cell population. Myofiber-associated satellite cells expressing a scrambled shRNA proliferate rapidly until 4d in culture, at which point they begin to lose PAX7, terminally differentiate, and become indistinguishable from untreated cells (Figure 6N) (Cornelison et al., 2001; Olguin and Olwin, 2004; Olguin et al., 2007).

### AraC-Resistant Cells and Satellite-SP Cells Are Similar

We have previously reported that satellite-SP cells express *Sca1* and ABCG2; when transplanted, satellite-SP cells expand and engraft into the satellite cell niche, effectively repopulating the satellite cell compartment (Tanaka et al., 2009). To test for a relationship between satellite-SP cells and the AraC-resistant population, we asked if AraC-resistant cells express *Sca1* and *Abcg2*. Myofiber-associated Syndecan-4+ satellite cells, treated with AraC from 2d to 4d in culture, were fixed and scored for SCA1 and ABCG2 immunoreactivity. In untreated cultures, SCA1+ and ABCG2+ cells comprise only a small percentage of Syndecan-4+ cells after 4d in culture (Figure 7A, 7B, S6A, and S6B). In marked contrast, the majority of AraC-resistant satellite cells, which are PAX7+/MYOD– and quiescent, are also SCA1+ (Figures 7A and 7C) and ABCG2+ (Figures S6A and S6C). Since AraC-resistant cells possess satellite-SP cell markers, we asked if SCA1+ cells were PAX7+/MYOD–. We found that virtually all SCA1+ cells are PAX7+/MYOD– (Figures 7D, 7E, and 7H) while the proliferating PAX7+/MYOD+ myoblast population is SCA1– (Figures 7F, 7G, and 7H). Quantification of these populations revealed that a very small percentage of SCA1+ cells are MYOD+ (Figure 7H). Together, these data indicate that the AraC-resistant population and the satellite-SP population overlap and comprise the PAX7+/MYOD quiescent satellite cell population.

The involvement of satellite-SP cells in asymmetric cell division and the capacity of these cells to repopulate the satellite cell compartment after transplantation suggest that satellite cells and satellite-SP cells may possess distinct gene expression profiles, consistent with their phenotypes. We isolated the satellite-SP cells from the satellite cell population by FACS as previously described (Figures S6D and S6E) (Tanaka et al., 2009) and identified differentially expressed genes in these two populations using Affymetrix gene chip arrays. We then assembled a putative signaling network coupling the Par complex to p38α/β MAPK signaling using a combination of Ingenuity Pathway Analysis (IPA) and literature searches (Figures S6F and S6G and Table S1). The gene expression values obtained from the Affymetrix gene chips overlaid onto the signaling network permitted visualization of the

relative expression of genes in the satellite cell population devoid of satellite-SP cells (Figure S6F). The small GTPases, *Rac1*, *Cdc42*, and *p38*a *mapk* are the most highly expressed in the satellite cells, along with additional members of the p38α/β MAPK signaling pathway (Figure S6F and Table S2). To visualize the distinct expression profiles between satellite-SP cells and satellite cells, we superimposed the differences in gene expression values between the two populations onto the Par-MAPK signaling network (Figure S6G). As expected, members of the p38α/β MAPK pathway, including *p38*a, MKK4 (*Map2k4*), and MKK6 (*Map2k6*), are reduced in satellite-SP cells compared to satellite cells (Figure S6G and Table S2), while the RAC1 guanine nucleotide exchange factor *Tiam1* (van Leeuwen et al., 1995) and Cerebral Cavernous Malformation 2 (Ccm2) (Uhlik et al., 2003), a scaffold for RAC1, MEKK3 (*Map3k3*), and MKK3 (*Map2k3*), are elevated in satellite-SP cells compared to satellite cells (Figure S6G, Table S1, and Table S2) (van Leeuwen et al., 1995). These data further extend the differences between these cell types and identify potential signaling pathways for future analysis.

A prediction of our model for asymmetric generation of an AraC-resistant satellite-SP cell and a myoblast daughter is that pp38α/β MAPK and satellite-SP cell markers should be distributed opposite daughters in an asymmetrically dividing cell. Indeed, we observed that SCA1 and pp38α/β MAPK were asymmetrically distributed in opposite daughter cells during the first myofiber-associated satellite cell division in culture (Figure 7I, Movie S2). Thus, a subset of satellite cells appear to divide asymmetrically, producing one committed MYOD+ daughter cell and one stem cell daughter that reacquires a quiescent phenotype, are MYOD– and retain the satellite-SP cell identity.

## DISCUSSION

Regeneration of skeletal muscle following an external or exercise-induced injury is accompanied by replenishment of the satellite cell pool (Schultz, 1984). Satellite cells associated with isolated myofibers appear capable of self-renewal both in culture (Olguin and Olwin, 2004; Zammit et al., 2004) and in host muscle tissue when transplanted in vivo (Collins et al., 2005; Hall et al., 2010). We recently performed long-term serial transplantations of myofiber-associated satellite cells, demonstrating that these cells exhibit long-term self-renewal capacity (Hall et al., 2010). Whether all satellite cells possess the ability to self-renew or a subset of satellite cells function as stem cells is not known. Prior reports demonstrate heterogeneity in the satellite cell population (Zammit et al., 2004; Olguin and Olwin, 2004) that is reflected upon transplantation in vivo (Kuang et al., 2007; Sacco et al., 2008; Tanaka et al., 2009), suggesting that a subset of satellite cells consists of a self-renewing progenitor. Consistent with the idea of a satellite cell progenitor population are observations that subsets of satellite cells display long-term BrdU retention (Shinin et al., 2006; Conboy et al., 2007; Tanaka et al., 2009; Rocheteau et al., 2012), divide asymmetrically (Kuang et al., 2007), and have an enhanced capacity for self-renewal when engrafted into a diseased or injured muscle (Montarras et al., 2005; Sacco et al., 2008; Tanaka et al., 2009).

When attempting to identify a potential satellite cell progenitor, we asked if any satellite cells maintained quiescence upon explant into culture. We found that all satellite cells

respond uniformly by activating and entering S-phase after explant as dispersed culture or as myofiber-associated satellite cells. It is not until after an initial division that BrdU-retaining, AraC-resistant cells (PAX7+/MYOD–/SCA1+) are generated. Thus, the initial satellite self-renewal event occurs during the first division after explant into culture. Because the AraC-resistant, BrdU-retaining cells are typically observed in isolation despite an initial division, it is likely that they arise by an asymmetric cell division, a behavior characteristic of the *Myf5*– satellite cell population (Kuang et al., 2007). This division produces a myoblast daughter cell, which rapidly undergoes further divisions, with the other daughter maintaining a satellite cell phenotype (quiescent, PAX7+/MYOD–/SCA1+). The AraC-resistant population we have identified has many features in common with the *Myf5*– population, as they are both daughters of asymmetric divisions that retain a quiescent satellite cell phenotype. Moreover, the AraC-resistant satellite cells can be restimulated in culture to produce both myoblast and satellite cell progeny, consistent with the stem cell behavior of *Myf5*– cells (Kuang et al., 2007) and satellite-SP cells (Tanaka et al., 2009).

To better understand the mechanisms involved in generating AraC-resistant cells, we identified a number of cell polarity genes whose expression is regulated during the initial cell division after satellite cell activation. The asymmetric distribution of the Par complex (Suzuki and Ohno, 2006) and its colocalization with pp38α/β MAPK was consistently observed in a fraction of dividing satellite cells, correlating strongly with observations of asymmetric MYOD expression between daughter satellite cells. We believe it is unlikely that pp38α/β MAPK asymmetry is artifactual because dividing cells with asymmetric pp38α/β MAPK contain uniform staining for pan-p38α/β MAPK and localize SCA1 to the opposite prospective daughter cell. These observations allow us to postulate a potential mechanism by which satellite-SP cells divide asymmetrically to produce a daughter cell committed to myogenesis and a quiescent satellite cell progenitor. A functional involvement of the Par complex in regulating self-renewal of satellite cells and myogenesis was confirmed by a number of independent experiments. First, we demonstrated that p38α/β MAPK signaling, MYOD transcriptional activity, and myogenic commitment require PKCλ. Second, we knocked down *Par-3*, eliminating the asymmetric distribution of p38α/β MAPK and enhancing the production of quiescent satellite cells. While we observed low levels of PAR-3 in the majority of mitotic cells by immunofluorescence, the knockdown of *Par-3* affected the entire population, suggesting that PAR-3 is either functional at low levels or that the protein is transiently upregulated or localized to the cell membrane, presumably during cell division. Our data support a mechanism for activation or sequestration of p38α/β MAPK by the Par complex to impose asymmetry, regulating satellite cell activity and satellite cell fate. Polar distribution of the Par complex (Suzuki and Ohno, 2006), which orients the plane of division and reinforces differential daughter cell fates through downstream signaling pathways, is evolutionarily conserved (Knoblich, 2008).

Linking asymmetric division of satellite cells to an injury response could allow the severity of the injury to balance asymmetric and symmetric division, ensuring that sufficient numbers of satellite cells self-renew. In our current working model (see Graphical Abstract online), we propose that asymmetric activation of p38α/β MAPK induces *MyoD* in the daughter cell receiving the Par/p38α/β MAPK complex, committing that daughter to

myogenesis. The other daughter cell, which expresses satellite-SP markers, adopts a quiescent satellite cell phenotype, preserving the stem cell population for the continued maintenance and repair of skeletal muscle tissue.

## EXPERIMENTAL PROCEDURES

### Immunofluorescence Analysis

Immunofluorescence was performed as described in the Supplemental Experimental Procedures. For the proximity ligation assay, samples were incubated with antibody at the concentrations listed in the Supplemental Experimental Procedures. Secondary antibody incubation and Duolink proximity ligation assay were performed according to manufacturer's protocol (Olink Bioscience).

Myofiber-associated cells were scored by counting the numbers of cells per fiber or cells per millimeter of fiber. To score asymmetric protein distribution, all dividing cells on ≥75 cultured myofibers were analyzed or, when following transfection, all mCherry+, dividing cells on ≥750 fibers were counted. Mitotic cells were identified by pH3 immunoreactivity or DAPI staining indicative of mitotic DNA. Nuclear levels of PAX7 and MYOD fluorescence were measured in SlideBook 4.0 by subtracting the average cytoplasmic intensity (determined by Syndecan-4) from the average nuclear intensity (determined by overlap with DAPI staining). Daughter cell pairs containing one cell with negative nuclear staining and one cell with staining one standard deviation greater than the negative cell were scored as asymmetric. Confocal images were displayed as 3D reconstructions or slices through a 3D reconstruction generated in Volocity 5.0 (Improvision). Two-tailed, unpaired t tests were used to generate p values.

### Arrays and Analysis

To generate the gene expression heat maps during the muscle injury time course, previously generated gene chip array data (Tanaka et al., 2009) were analyzed using Spotfire Decisionsite Software after normalization by GCRMA.

A putative PAR-3/p38α/β MAPK signaling network was generated using IPA combined with literature searches. To display expression levels on the network, the IPA shape was colored black and the opacity was determined by the average $\log_{10}$ expression of the most highly represented probe set for that gene, where most highly expressed gene was set to 100, and the lowest, to 0. To display differential expression between satellite cells and satellite-SP cells, genes with a probe set showing at least a 2-fold change in expression and $p < 0.02$ were colored green (increase in satellite-SP cells) or red (increase in non-SP satellite cells). The intensity of color (red or green) reflects the difference in expression between the two cell populations with a higher intensity indicating a greater difference in expression.

### PKCλ and Par-3 Knockdown

Expression vectors encoding sense and antisense PKCλ fragments are described elsewhere (Kampfer et al., 1998; Bandyopadhyay et al., 1999). DNA was transfected into MM14 cells as described in the Supplemental Experimental Procedures. Validated shRNAs targeting

*Par-3* (Sigma-Aldrich, TRCN0000094400, TRCN0000094401) were cloned into vectors coexpressing mCherry from a separate promoter. Myofiber-associated satellite cells were transfected as described in the Supplemental Experimental Procedures directly after isolation. Expression of mCherry was detected as early as 18 hr after transfection.

## Supplementary Material

Refer to Web version on PubMed Central for supplementary material.

## Acknowledgments

We thank Tiffany Antwine and Nicole Dalla Betta for technical assistance. The work was supported by grants from the NIH (AR049446) and the Muscular Dystrophy Association to B.B.O.

## REFERENCES

Aguirre-Ghiso JA, Estrada Y, Liu D, Ossowski L. ERK(MAPK) activity as a determinant of tumor growth and dormancy; regulation by p38(SAPK). Cancer Res. 2003; 63:1684–1695. [PubMed: 12670923]

Bandyopadhyay G, Standaert ML, Kikkawa U, Ono Y, Moscat J, Farese RV. Effects of transiently expressed atypical (zeta, lambda), conventional (alpha, beta) and novel (delta, epsilon) protein kinase C isoforms on insulin-stimulated translocation of epitope-tagged GLUT4 glucose transporters in rat adipocytes: specific interchangeable effects of protein kinases C-zeta and C-lambda. Biochem. J. 1999; 337:461–470. [PubMed: 9895289]

Collins CA, Olsen I, Zammit PS, Heslop L, Petrie A, Partridge TA, Morgan JE. Stem cell function, self-renewal, and behavioral heterogeneity of cells from the adult muscle satellite cell niche. Cell. 2005; 122:289–301. [PubMed: 16051152]

Conboy MJ, Karasov AO, Rando TA. High incidence of non-random template strand segregation and asymmetric fate determination in dividing stem cells and their progeny. PLoS Biol. 2007; 5:e102. [PubMed: 17439301]

Cornelison DD, Filla MS, Stanley HM, Rapraeger AC, Olwin BB. Syndecan-3 and syndecan-4 specifically mark skeletal muscle satellite cells and are implicated in satellite cell maintenance and muscle regeneration. Dev. Biol. 2001; 239:79–94. [PubMed: 11784020]

Doe CQ. Cell polarity: the PARty expands. Nat. Cell Biol. 2001; 3:E7–E9. [PubMed: 11146637]

Doe CQ. Neural stem cells: balancing self-renewal with differentiation. Development. 2008; 135:1575–1587. [PubMed: 18356248]

Furth JJ, Cohen SS. Inhibition of mammalian DNA polymerase by the 5′-triphosphate of 1-beta-d-arabinofuranosylcytosine and the 5′-triphosphate of 9-beta-d-arabinofuranoxyladenine. Cancer Res. 1968; 28:2061–2067. [PubMed: 5754840]

Giebel B, Bruns I. Self-renewal versus differentiation in hematopoietic stem and progenitor cells: a focus on asymmetric cell divisions. Curr. Stem Cell Res. Ther. 2008; 3:9–16. [PubMed: 18220918]

Hall JK, Banks GB, Chamberlain JS, Olwin BB. Prevention of muscle aging by myofiber-associated satellite cell transplantation. Sci. Transl. Med. 2010; 2:57ra83.

Jones NC, Tyner KJ, Nibarger L, Stanley HM, Cornelison DD, Fedorov YV, Olwin BB. The p38alpha/beta MAPK functions as a molecular switch to activate the quiescent satellite cell. J. Cell Biol. 2005; 169:105–116. [PubMed: 15824134]

Kampfer S, Hellbert K, Villunger A, Doppler W, Baier G, Grunicke HH, Uberall F, Bandyopadhyay G, Standaert ML, Kikkawa U, et al. Transcriptional activation of c-fos by oncogenic Ha-Ras in mouse mammary epithelial cells requires the combined activities of PKC-lambda, epsilon and zeta. Embo J. 1998; 17:4046–4055. [PubMed: 9670019]

Knoblich JA. Mechanisms of asymmetric stem cell division. Cell. 2008; 132:583–597. [PubMed: 18295577]

Kuang S, Kuroda K, Le Grand F, Rudnicki MA. Asymmetric self-renewal and commitment of satellite stem cells in muscle. Cell. 2007; 129:999–1010. [PubMed: 17540178]

Le Grand F, Jones AE, Seale V, Scimè A, Rudnicki MA. Wnt7a activates the planar cell polarity pathway to drive the symmetric expansion of satellite stem cells. Cell Stem Cell. 2009; 4:535–547. [PubMed: 19497282]

Lin H. Cell biology of stem cells: an enigma of asymmetry and self-renewal. J. Cell Biol. 2008; 180:257–260. [PubMed: 18227277]

Lin D, Edwards AS, Fawcett JP, Mbamalu G, Scott JD, Pawson T. A mammalian PAR-3-PAR-6 complex implicated in Cdc42/Rac1 and aPKC signalling and cell polarity. Nat. Cell Biol. 2000; 2:540–547. [PubMed: 10934475]

Lyons AB. Divided we stand: tracking cell proliferation with carboxyfluorescein diacetate succinimidyl ester. Immunol. Cell Biol. 1999; 77:509–515. [PubMed: 10571671]

Mauro A. Satellite cell of skeletal muscle fibers. J. Biophys. Biochem. Cytol. 1961; 9:493–495. [PubMed: 13768451]

Montarras D, Morgan J, Collins C, Relaix F, Zaffran S, Cumano A, Partridge T, Buckingham M. Direct isolation of satellite cells for skeletal muscle regeneration. Science. 2005; 309:2064–2067. [PubMed: 16141372]

Olguin HC, Olwin BB. Pax-7 up-regulation inhibits myogenesis and cell cycle progression in satellite cells: a potential mechanism for self-renewal. Dev. Biol. 2004; 275:375–388. [PubMed: 15501225]

Olguin HC, Yang Z, Tapscott SJ, Olwin BB. Reciprocal inhibition between Pax7 and muscle regulatory factors modulates myogenic cell fate determination. J. Cell Biol. 2007; 177:769–779. [PubMed: 17548510]

Park JK, Lee JS, Lee HH, Choi IS, Park SD. Accumulation of polycyclic aromatic hydrocarbon-induced single strand breaks is attributed to slower rejoining processes by DNA polymerase inhibitor, cytosine arabino-side in CHO-K1 cells. Life Sci. 1991; 48:1255–1261. [PubMed: 2002753]

Pisconti A, Cornelison DD, Olguín HC, Antwine TL, Olwin BB. Syndecan-3 and Notch cooperate in regulating adult myogenesis. J. Cell Biol. 2010; 190:427–441. [PubMed: 20696709]

Rocheteau P, Gayraud-Morel B, Siegl-Cachedenier I, Blasco MA, Tajbakhsh S. A subpopulation of adult skeletal muscle stem cells retains all template DNA strands after cell division. Cell. 2012; 148:112–125. [PubMed: 22265406]

Sacco A, Doyonnas R, Kraft P, Vitorovic S, Blau HM. Self-renewal and expansion of single transplanted muscle stem cells. Nature. 2008; 456:502–506. [PubMed: 18806774]

Schultz E. A quantitative study of satellite cells in regenerated soleus and extensor digitorum longus muscles. Anat. Rec. 1984; 208:501–506. [PubMed: 6731859]

Schultz E, McCormick KM. Skeletal muscle satellite cells. Rev. Physiol. Biochem. Pharmacol. 1994; 123:213–257. [PubMed: 8209136]

Seale P, Sabourin LA, Girgis-Gabardo A, Mansouri A, Gruss P, Rudnicki MA. Pax7 is required for the specification of myogenic satellite cells. Cell. 2000; 102:777–786. [PubMed: 11030621]

Sekizawa K, Suzuki T, Kishi K. Cytogenetic study of the induction mechanism of chromosome-type aberrations by 1-beta-D-arabinofuranosylcytosine. Mutat. Res. 2007; 619:1–8. [PubMed: 17397878]

Shinin V, Gayraud-Morel B, Gomès D, Tajbakhsh S. Asymmetric division and cosegregation of template DNA strands in adult muscle satellite cells. Nat. Cell Biol. 2006; 8:677–687. [PubMed: 16799552]

Suzuki A, Ohno S. The PAR-aPKC system: lessons in polarity. J. Cell Sci. 2006; 119:979–987. [PubMed: 16525119]

Tabuse Y, Izumi Y, Piano F, Kemphues KJ, Miwa J, Ohno S. Atypical protein kinase C cooperates with PAR-3 to establish embryonic polarity in Caenorhabditis elegans. Development. 1998; 125:3607–3614. [PubMed: 9716526]

Tanaka KK, Hall JK, Troy AA, Cornelison DD, Majka SM, Olwin BB. Syndecan-4-expressing muscle progenitor cells in the SP engraft as satellite cells during muscle regeneration. Cell Stem Cell. 2009; 4:217–225. [PubMed: 19265661]

Uhlik MT, Abell AN, Johnson NL, Sun W, Cuevas BD, Lobel-Rice KE, Horne EA, Dell'Acqua ML, Johnson GL. Rac-MEKK3-MKK3 scaffolding for p38 MAPK activation during hyperosmotic shock. Nat. Cell Biol. 2003; 5:1104–1110. [PubMed: 14634666]

van der Flier LG, Clevers H. Stem cells, self-renewal, and differentiation in the intestinal epithelium. Annu. Rev. Physiol. 2009; 71:241–260. [PubMed: 18808327]

van Leeuwen FN, van der Kammen RA, Habets GG, Collard JG. Oncogenic activity of Tiam1 and Rac1 in NIH3T3 cells. Oncogene. 1995; 11:2215–2221. [PubMed: 8570171]

Yablonka-Reuveni Z, Rivera AJ. Temporal expression of regulatory and structural muscle proteins during myogenesis of satellite cells on isolated adult rat fibers. Dev. Biol. 1994; 164:588–603. [PubMed: 7913900]

Zammit PS, Golding JP, Nagata Y, Hudon V, Partridge TA, Beauchamp JR. Muscle satellite cells adopt divergent fates: a mechanism for self-renewal? J. Cell Biol. 2004; 166:347–357. [PubMed: 15277541]

Zdunski D, Ilan J. The effect of cytosine arabinoside on the synthesis of rapidly labeled RNA during DNA replicating and non-DNA replicating periods of the cell cycle. Cell Differ. 1980; 9:181–191. [PubMed: 6156009]

Zhang YV, Cheong J, Ciapurin N, McDermitt DJ, Tumbar T. Distinct self-renewal and differentiation phases in the niche of infrequently dividing hair follicle stem cells. Cell Stem Cell. 2009; 5:267–278. [PubMed: 19664980]

Zhang K, Sha J, Harter ML. Activation of Cdc6 by MyoD is associated with the expansion of quiescent myogenic satellite cells. J. Cell Biol. 2010; 188:39–48. [PubMed: 20048262]

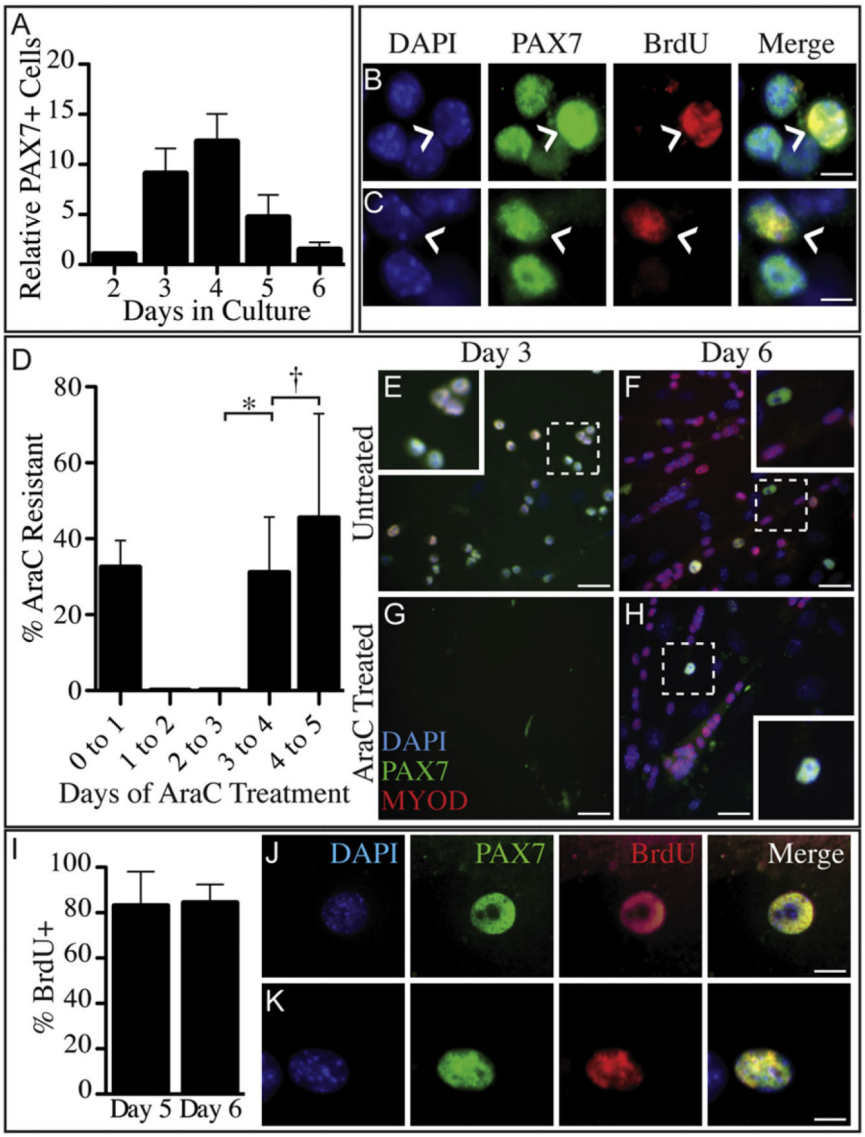


**Figure 1. A Subset of Primary Satellite Cells Withdraws from the Cell Cycle after an Initial Division following Activation**

PAX7+ (green; B, C, E–H, J, and K), MYOD+ (red; B, C, E–H, J, and K) primary myoblasts initially increase in culture (A and E) before declining in number as cells lose *Pax7* expression and commit to differentiation (A and F). When treated from 0d to 2d in culture with BrdU, a subset of PAX7+ (green) primary myoblasts retain BrdU (red) through 5d (B, caret, 13%) and 6d (C, caret, 37%) of culture. All PAX7+ cells are AraC sensitive during the first division (D and G) but 40%–50% of PAX7+ cells (green) are AraC resistant when treated from 3d to 4d or 4d to 5d with AraC (D and H). All AraC-resistant cells cycle at least once before cell cycle withdrawal as these cells incorporate and retain BrdU when provided with BrdU from 0d to 2d in culture and subsequently treated with AraC from 3d to 4d in culture (I and J) or from 4d to 5d in culture (I and K), followed by a 1d chase in the absence of AraC. Error bars represent standard error of the mean. (*$p < 0.01$; y not significant). White scale bars indicate 5 μm (B, C, J, and K) or 30 μm (E–H). See Figure S1.

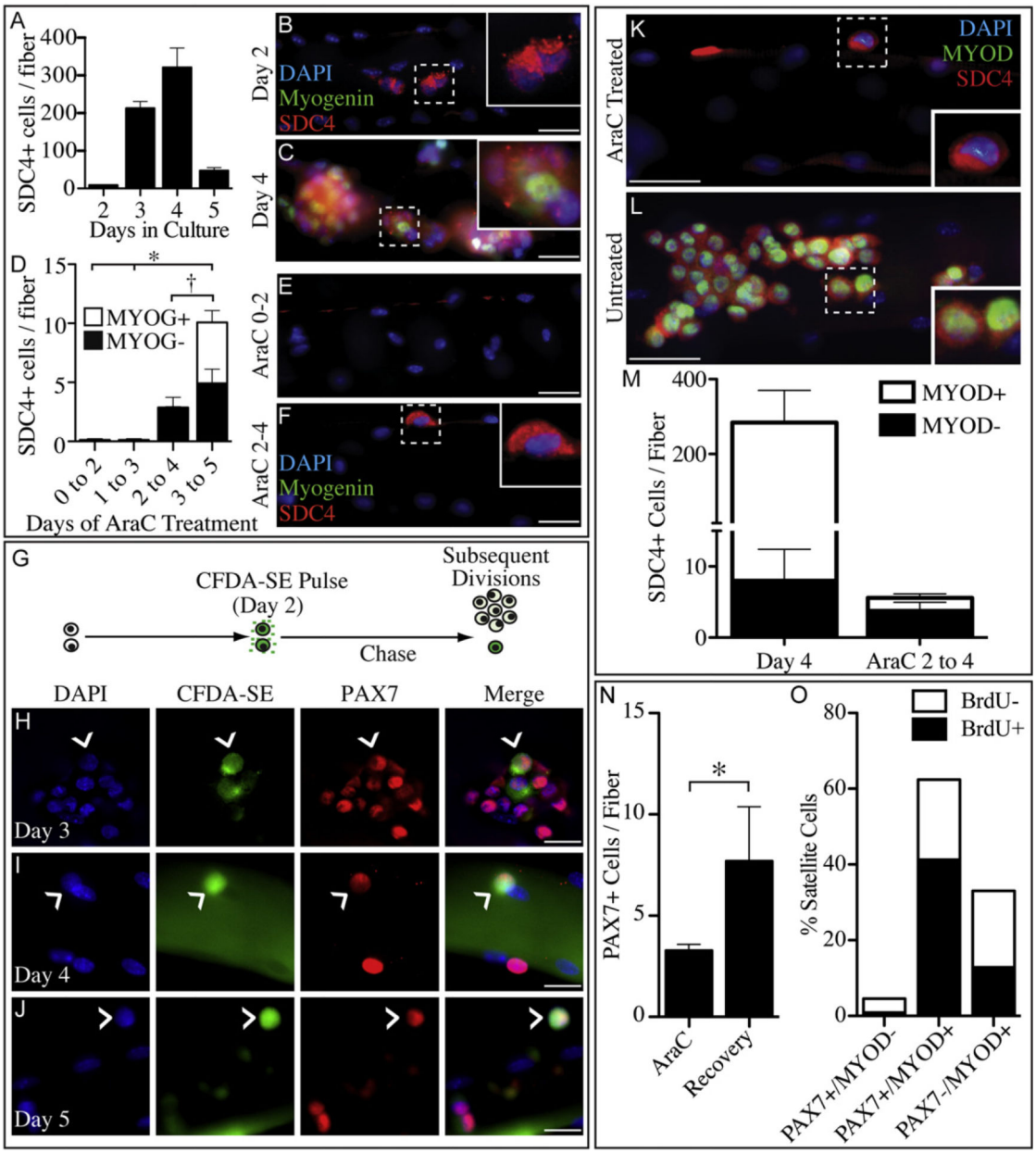


**Figure 2. MYOD Is Asymmetric in a Subset of Myofiber-Associated Satellite Cells that Withdraws from the Cell Cycle during the First Division**

Myofiber-associated Syndecan-4+ satellite cells divide by 36–48 hr postisolation, then rapidly increase in number (A), whereas in 2d cultures, Syndecan-4+ (B, Sdc4, red) cells are present in pairs with no Myogenin+ cells (B, green). By 4d these expand to large colonies containing both Myogenin+ and Myogenin– cells (C). All myofiber-associated Syndecan-4+ cells are AraC sensitive during the first 2d of culture (D and E), but AraC treatments from either 2d to 4d or 3d to 5d reveal an AraC-resistant, undifferentiated population (D and F) that does not increase after 2d in culture (D) and is predominantly composed of single cells (F). A similar nondividing Syndecan-4+ population of myofiber-associated cells is revealed by CFDA-SE retention (G) when treated for 15 min with CFDA and cultured in the absence

of CFDA for 3d (H), 4d (I), or 5d (J). MYOD immunofluorescence is undetectable in the majority of myofiber-associated cells after AraC treatment from 2d to 4d (K and M, green). In contrast, the majority of untreated myofiber-associated cells are MYOD+ (L and M). AraC-resistant cells are capable of regenerating myoblasts and satellite cells since myofibers treated with AraC from 3d to 5d and subsequently cultured in the absence of AraC until 8d have an increased number of PAX7+ cells when compared to fibers fixed directly after AraC treatment (N). AraC-resistant cells generate PAX7+/MYOD–, PAX7+/MYOD+, and PAX7–/MYOD+ progeny and incorporate BrdU when treated for 5 hr prior to fixation (O), similar to untreated cells (C and L). Error bars represent standard error of the mean (*$p < 0.02$; † denotes no significant difference for MYOG– bars only). White scale bars indicate 30 μm (B–F, K, and L) and 20 μm (H–J). See Figures S1 and S2.

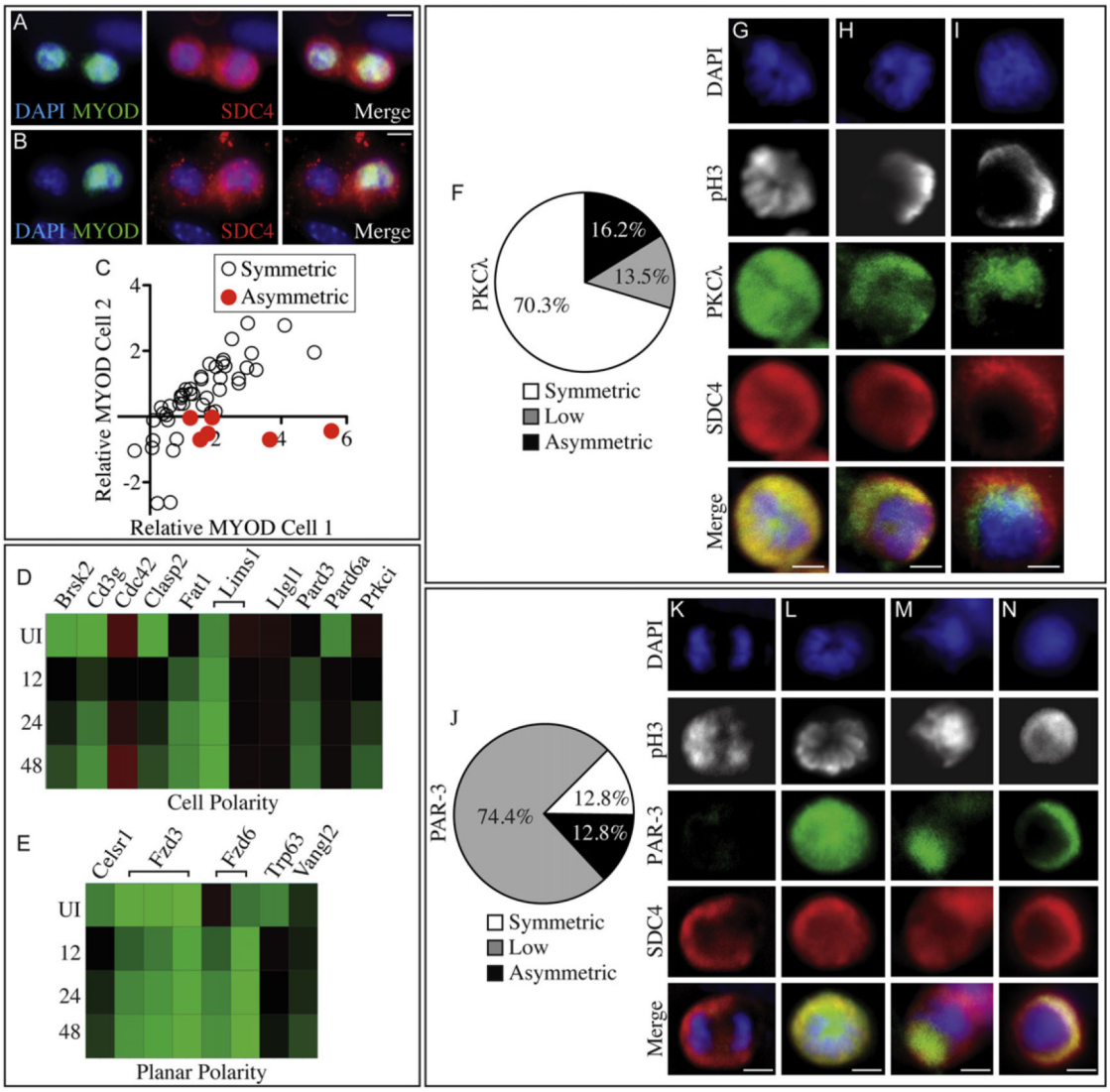


**Figure 3. Par Complex Localization Is Asymmetric in a Subset of Satellite Cells during the First Division after Activation**

While the majority of Syndecan-4+ cell pairs have equivalent levels of MYOD immunofluorescence at 48 hr (A and C, orange circle), 12% of cell pairs have asymmetric MYOD (B and C, orange circle). Each circle represents an individual pair of daughter cells with axes indicating the relative nuclear MYOD fluorescence intensity above cytoplasmic levels of one cell in the pair (C). Asymmetric (red) pairs have no detectable MYOD in one cell of each pair (C, orange circle). Heat maps derived from Affymetrix expression data obtained from Syndecan-4+ cells isolated from uninjured (UI) muscle tissue and 12 hr, 24 hr, and 48 hr postinjury and queried for the presence of GO annotations for cell polarity (GO:0007163, D) and planar polarity (GO:0001736, E) show changes in relative expression during the first cell division. At 36 hr of culture, mitotic cells were scored for PKCλ asymmetry (F), where the majority of mitotic (G–I, K–N, phosphohistone-3 immunoreactive, white) Syndecan-4+ (G–I and K–N, red) cells exhibit uniform PKCλ distribution (F and G green) and a minority exhibit asymmetric PKCλ localization (F, H, and

I, green, n = 37). When examined for the PAR-3 protein, the majority of mitotic, Syndecan-4+ cells have very low levels of PAR-3 (J and K, green), while a minority show either uniform localization of PAR-3 (J and L, green) or asymmetrically localized PAR-3 (J, M, and N, green, n = 39). White scale bars indicate 5 μm. See Figure S3.

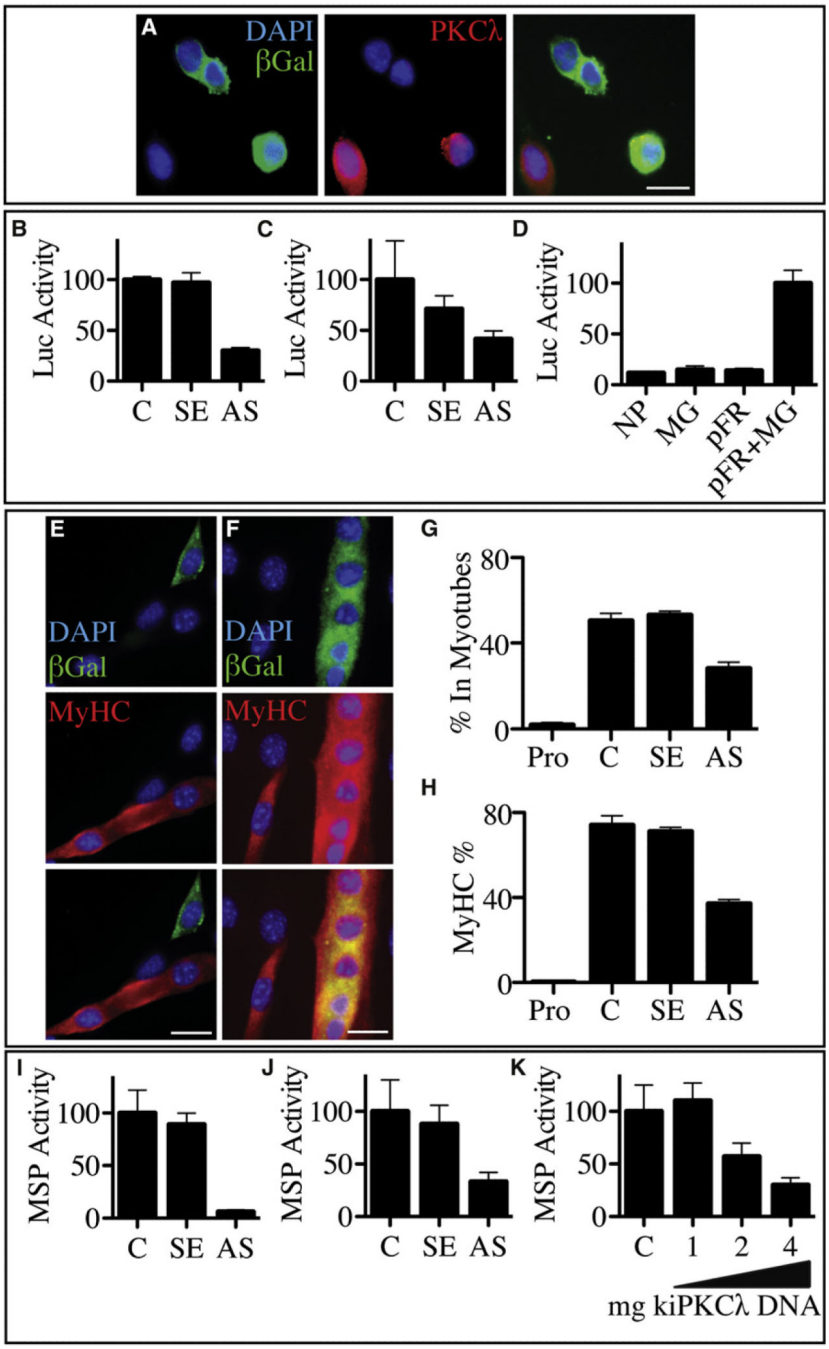


**Figure 4. PKCλ Is Required for MYOD Activity and Myogenesis**

MM14 cells cotransfected with expression vectors encoding LacZ (A, green) and an antisense PKCλ construct show loss of PKCλ protein (A, red). MYOD transcriptional activity is reduced when MM14 cells (B) or primary satellite cells (C) are cotransfected with the MYOD-Gal4/pFR-Lucif-erase reporter system and an antisense PKCλ construct (AS) compared to activity levels after transfection with either an empty vector (Control) or sense PKCλ construct (B and C, and Figure SE). Comparison of mock transfection (NP), transfection individual components of the MYOD-Gal4/ pFR-Luciferase reporter system

(MG, pFR), or transfection of both plasmids into MM14 cells demonstrates that the Gal4 reporter system effectively measures MYOD-dependent transcription (D). MM14 cells cotransfected with a LacZ expression vector and antisense PKCλ vector (E) under differentiation conditions fail to express MyHC (red) in b-galactosidase+ (green) cells when compared to those transfected with the sense PKCλ vector (F). When quantified, a 2-fold reduction in fused myonuclei (G) or in MyHC+ cells (H) is observed for cells transfected with antisense PKCλ relative to those transfected with sense PKCλ, where little differentiation is detected in cells grown under proliferative conditions (Pro.). Similarly, muscle-specific gene expression in MM14 cells in the presence of the antisense PKCλ plasmid was reduced 20-fold compared to that in cells transfected with either an empty vector (pcDNA) or the sense PKCλ plasmid after 48 hr in differentiation conditions (I). Primary myoblasts derived from satellite cells show a similar reduction in muscle-specific gene expression in the presence of the antisense PKCλ plasmid (J). PKCλ kinase activity is required for muscle-specific gene expression in MM14 cells as increasing amounts of a kinase inactive (ki) PKCλ encoding plasmid reduces muscle-specific reporter activity in MM14 cells (K). Error bars represent the standard error of the mean. White scale bars indicate 20 μm. See Figure S4.

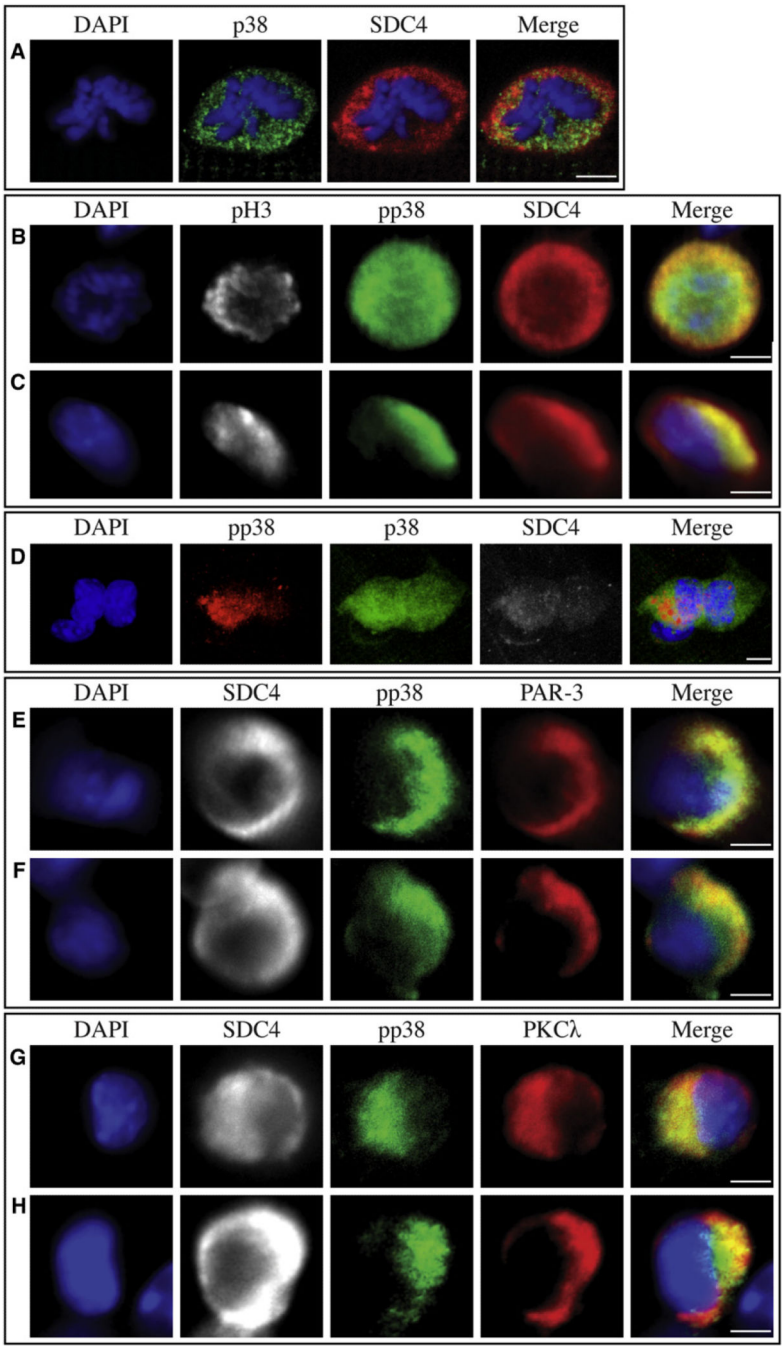


**Figure 5. pp38α/β MAPK Is Asymmetrically Distributed in a Subset of Satellite Cells and Colocalizes with PAR-3 and PKCλ**

p38α/β MAPK immunoreactivity is symmetric (A, green) in all myofiber-associated, Syndecan-4+ (A– C, red) cells at 36 hr in culture. While the majority of mitotic (B and C, phosphohistone-3, white) Syndecan-4+ (B and C, red) cells display uniform immunoreactivity for the active, phosphorylated p38α/β MAPK (B, pp38α/β MAPK, green), it is asymmetrically localized in a subset of mitotic satellite cells (C–H), colocalizing with only a subset of p38α/β MAPK (D, red). All myofiber-associated Syndecan-4+ (D–H, white) cells with asymmetric pp38α/β MAPK show colocalization of pp38α/β MAPK

immunofluorescence with PAR-3 immunofluorescence(E and F,red) and PKCλ immunofluorescence (G and H, red). White scale bars indicate 5 μm.

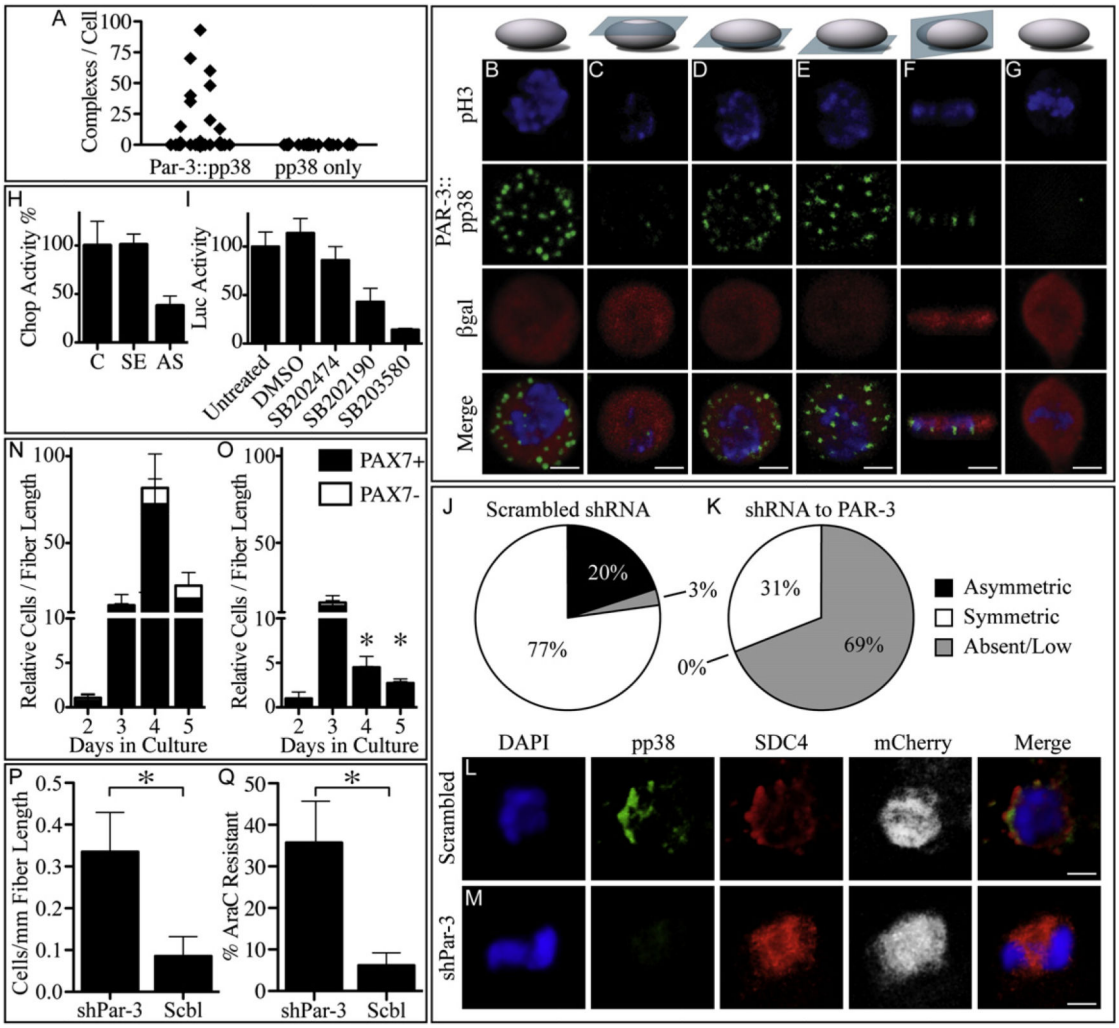


**Figure 6. The Par Complex Is Necessary for Generating Transit Amplifying Myoblasts and Is Present in a Complex with pp38α/β MAPK**

PLAs identify complexes of pp38α/β MAPK and PAR-3 (B–G, green) in a subset of mitotic (B–G, phosphohistone-3, blue), *Pax7*+ (B–G, $Pax7^{tmLacZ}$/+ bgal, red) satellite cells (A), displayed by 3D confocal reconstruction (B). Complexes of PAR-3 and pp38α/β MAPK localize to the substrate contact surface (D–F) and not the medium exposed surface (C) in mitotic, *Pax7*+ satellite cells (see Movie S1). Complexes are not detected in PLAs if one primary antibody is omitted (A and G). The kinase activity of p38α/β MAPK, as measured by a CHOP reporter assay, is reduced 2.5-fold upon transfection of the antisense PKCλ plasmid when compared to mock transfected (C) or sense PKCλ plasmid transfected (SE) MM14 cells (H). Inhibition of p38 activity by p38 MAPK inhibitors SB202190 and SB203580 reduces MYOD transcriptional activity in MM14 cells transfected with the MYOD-Gal4/pFR-Luciferase reporter system compared to untreated cells, cells treated with DMSO, and cells treated with the inactive drug analog SB202474 (I). In dividing myofiber-associated cells, knockdown of *Par-3* eradicates most of the pp38α/β MAPK immunoreactivity and eliminates all detectable asymmetric pp38α/β MAPK (K and M, n = 29) where a subset of dividing myofiber-associated satellite cells (Syndecan-4, red, L and

M) expressing a scrambled shRNA (mCherry, white, L and M) asymmetrically localize pp38α/β MAPK (J and L, n = 35). Assuming a 10%–15% transfection efficiency, with an analysis at 36 hr, prior to or during the first division in culture with ~5% undergoing mitosis and 8 satellite cells/myofiber we should observe ~40 mitotic satellite cells per 750 myofibers, consistent with our observations (J–M). Control myofiber-associated satellite cells expressing a scrambled shRNA proliferate until 4d in culture when they begin terminal differentiation and lose *Pax7* expression (N), whereas myofiber-associated satellite cells expressing a *Par-3* shRNA show reduced proliferation and no differentiation (O). A concomitant increase in the number and percentage of quiescent cells at 3d is observed in satellite cells transfected with the *Par-3* shRNA, compared to that of a scrambled shRNA transfected control, because they display increased survival following an AraC treatment from 3d to 5d (P and Q). Error bars represent the standard error of the mean; *$p < 0.01$. White scale bars indicate 5 μm. See Figure S5.

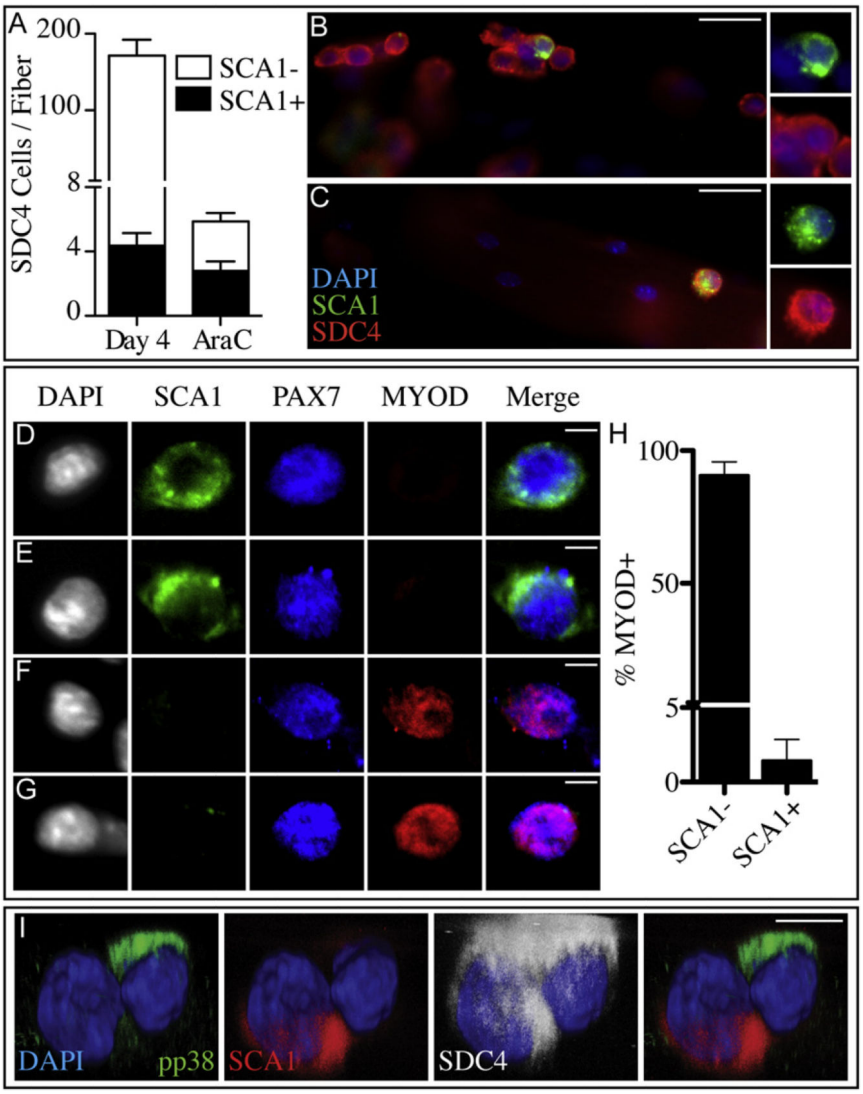


**Figure 7. The AraC-Resistant Cells Comprise the Satellite-SP Stem Cell Population**

A minority of myofiber-associated, Syndecan-4+ cells expresses the satellite-SP cell marker SCA1 at 4d of culture (A and B). In contrast, after AraC treatment the SCA1+ myofiber-associated cell population is increased 19-fold (A and C). After the first division following activation, myofiber-associated SCA1+ cells are PAX7+/MYOD– (D and E), while SCA1– cells are PAX7+/MYOD+ (F and G) and, when quantified, we found that <2% of the SCA1+ AraC-resistant population was MYOD+ (H). During asymmetric division, a myofiber-associated satellite cell (I) localizes the satellite-SP cell marker SCA1 (red) to one prospective daughter cell and localizes the promyogenic pp38α/β MAPK (green) to the opposite prospective daughter cell (I, see Movie S2). Error bars represent the standard error of the mean. White scale bars indicate 5 μm (D–G) or 30 μm (B and C). See Figure S6.